THE JOURNAL OF BIOLOGICAL CHEMISTRY VOL. 287, NO. 18, pp. 14912–14922, April 27, 2012

β-Actin-binding Complementarity-determining Region 2 of Variable Heavy Chain from Monoclonal Antibody C7 Induces Apoptosis in Several Human Tumor Cells and Is Protective against Metastatic Melanoma*[S]

Received for publication, November 9, 2011, and in revised form, February 9, 2012 Published, JBC Papers in Press, February 13, 2012, DOI 10.1074/jbc.M111.322362

Denise C. Arruda[‡], Luana C. P. Santos[‡], Filipe M. Melo[‡], Felipe V. Pereira[‡], Carlos R. Figueiredo[‡], Alisson L. Matsuo[‡§], Renato A. Mortara[¶1], Maria A. Juliano[‖1], Elaine G. Rodrigues[‡1], Andrey S. Dobroff[**], Luciano Polonelli[‡‡], and Luiz R. Travassos[‡§1,2]

*From the [‡]Experimental Oncology Unit (UNONEX), [¶]Division of Parasitology, and [‖]Department of Biophysics, Universidade Federal de São Paulo (UNIFESP), São Paulo SP 04023-062, Brazil, [§]Recepta Biopharma, São Paulo, SP 04533-014, Brazil, the **David H. Koch Center, the University of Texas M. D. Anderson Cancer Center, Houston, Texas 77030, and the [‡‡]Universitá degli Studi di Parma, Parma 43121, Italy*

Background: Immunoglobulin complementarity-determining region (CDR) peptides frequently display antitumor activities.
Results: Monoclonal antibody C7 CDR-H2 binds to β-actin and induces polymerization, F-actin stabilization, and tumor cell death.
Conclusion: Alterations of actin dynamics trigger reactive oxygen species and tumor cell apoptosis.
Significance: The *in vitro* apoptotic effect and *in vivo* antimetastatic activity of peptide C7H2 makes it a candidate to be developed as an anticancer drug.

Complementarity-determining regions (CDRs) from monoclonal antibodies tested as synthetic peptides display anti-infective and antitumor activities, independent of the specificity of the native antibody. Previously, we have shown that the synthetic peptide C7H2, based on the heavy chain CDR 2 from monoclonal antibody C7, a mAb directed to a mannoprotein of *Candida albicans*, significantly reduced B16F10 melanoma growth and lung colony formation by triggering tumor apoptosis. The mechanism, however, by which C7H2 induced apoptosis in tumor cells remained unknown. Here, we demonstrate that C7H2 interacts with components of the tumor cells cytoskeleton, being rapidly internalized after binding to the tumor cell surface. Mass spectrometry analysis and *in vitro* validation revealed that β-actin is the receptor of C7H2 in the tumor cells. C7H2 induces β-actin polymerization and F-actin stabilization, linked with abundant generation of superoxide anions and apoptosis. Major phenotypes following peptide binding were chromatin condensation, DNA fragmentation, annexin V binding, lamin disruption, caspase 8 and 3 activation, and organelle alterations. Finally, we evaluated the cytotoxic efficacy of C7H2 in a panel of human tumor cell lines. All tumor cell lines studied were equally susceptible to C7H2 *in vitro*. The C7H2 amide without further derivatization significantly reduced lung metastasis of mice endovenously challenged with B16F10-Nex2 melanoma cells. No significant cytotoxicity was observed toward nontumorigenic cell lines on short incubation *in vitro* or in naïve mice injected with a high dose of the peptide. We believe that C7H2 is a promising peptide to be developed as an anticancer drug.

Natural and synthetic peptides have been associated with antitumor effects and have been studied as potential drug candidates (1). Peptides exert direct cytotoxic activities causing necrosis, apoptosis, function-blocking effects, and inhibition of angiogenesis. Indirect activities are related mainly to stimulation of the immune system to eliminate tumor cells (2). Their advantages and similarities with chemotherapeutic antibodies are based on the high affinity and specificity for target tissues, low toxicity, and good penetration (1, 3).

Polonelli *et al.* (4) found that linear peptide fragments from an anti-idiotypic antibody had biological activities similar to the original antigen, a killer toxin from *Pichia anomala*. An engineered peptide consisting of seven amino acids of the framework sequence and three amino acids of the V_L[3] complementarity-determining region (CDR) 1 (L1) domain with one substitution (A1E) showed the maximum activity and was called killer peptide. The killer peptide proved to be cytotoxic to a number of fungal species, protozoa, bacteria, and viruses (5–9) but was inactive in mammalian cells. The concept that internal sequences of both chains of immunoglobulins, inde-

* This work was supported by Fundação de Amparo a Pesquisa do Estado de São Paulo (Fapesp) Grants 06/50634-2 and 10/51423-0.
[S] This article contains supplemental Figs. S1–S6.
[1] Recipients of career fellowships from the Brazilian National Research Council (CNPq).
[2] To whom correspondence should be addressed: Unidade de Oncologia Experimental (UNONEX), Universidade Federal de São Paulo (UNIFESP), Rua Botucatu 862, 8 andar, São Paulo, SP 04023-062, Brazil. Tel.: 55-11-50842991; Fax: 55-11-55715877; E-mail: travassos@unifesp.br.

[3] The abbreviations used are: V_L and V_H, light chain and heavy chain of immunoglobulin variable region; CDR, complementarity-determining region; DHE, dihydroethidium; F-actin, filamentous actin; G-actin, globular actin; ROS, reactive oxygen species.

pendently of antibody specificity, could have bioactive properties was further investigated using isolated CDRs tested as synthetic peptides (10). CDR peptides from different monoclonal antibodies showed anti-*Candida*, anti-HIV, and anti-melanoma activities. Anti-tumor CDRs were V_H CDR 2 (H2) and V_L CDR 1 (L1) from unrelated antibodies recognizing different antigens. Another CDR peptide (H3) showed immunomodulatory activity in macrophages (11) expanding the properties of these peptides with the perspective of future use in the development of medicinal drugs (12).

Of all CDRs, the V_H CDR 3 (H3) has unique properties: when tested as an isolated peptide it can, in many cases, reproduce major characteristics of the original antibody (13–15), thus being called a micro (mini) antibody. Recently, linear and cyclic extended (16) H3 peptides from two anti-melanoma (B16F10) mAbs (IgG and IgM) were shown to compete with the original mAb (A4 and A4M) for binding to melanoma cells. H3 from mAb A4 induced DNA degradation and inhibited tumor cell growth, similarly to the original mAb.

Both CDR peptides that were cytotoxic against *Candida albicans*, HIV-1 and murine melanoma (C7H2 and HuAL1) (10), represented prototypes of direct antitumor activity of peptides derived from IgGs. They were active against B16F10-Nex2 melanoma at EC_{50} 5.35×10^{-5} (C7H2) and 7.2×10^{-4} (HuAL1) and seemed to act by causing apoptosis as clearly shown in HL-60 cells. Although both peptides were protective against melanoma in a metastatic murine model, the mechanisms of cytotoxicity, including the molecular targets on tumor cells, seemed to differ considering their dissimilar amino acid sequences. Moreover, C7H2 showed maximal activity against *Candida* at 100 μg/ml compared with no activity by HuAL1 (10).

Presently, we have determined that C7H2 peptide induces apoptosis in tumor cell lines by affecting the dynamics and stability of the actin cytoskeleton. More importantly, we have uncovered β-actin as the molecular target of C7H2 peptide. Additionally, we established that underivatized C7H2 amide peptide induces apoptosis in several human tumor cell lines, with no significant short term cytotoxicity in nontumorigenic cell lines or in naïve mice at high concentration. Altogether, we propose that C7H2 is a strong candidate to be developed as a peptide-based anticancer agent.

EXPERIMENTAL PROCEDURES

Cell Lines—The clone B16F10-Nex2, a murine melanoma subline, was established at the Experimental Oncology Unit, Federal University of São Paulo, UNIFESP, as described elsewhere (17). The human tumor cell lines A2058 (melanoma), HCT-8 and LS180 (colon carcinoma), MCF-7, MDA and SKBR3 (breast carcinoma), and SiHa (cervical carcinoma) were provided by the Ludwig Institute for Cancer Research, São Paulo, Brazil. These cell lines were maintained in RPMI 1640 medium (Invitrogen) supplemented with 10 mM HEPES (Sigma-Aldrich), 24 mM sodium bicarbonate, 40 mg/liter gentamicin (Hipolabor, MG, Brazil), pH 7.2, and 10% fetal bovine serum (FBS). The human cervical carcinoma cell line HeLa and human glioblastoma cell line U87-MG, were provided by Hugo P. Monteiro, UNIFESP, and Osvaldo K. Okamoto, University of São Paulo, respectively. HeLa and U87-MG cells were maintained in DMEM (Invitrogen) supplemented as described above.

The human fibroblast cell line GM637 (18) and mouse embryonic fibroblasts were gifts from Luis F. Lima Reis, Hospital Sirio-Libanez, São Paulo. These cell lines were maintained in DMEM supplemented as described above. Rabbit aortic endothelial cells (19), provided by H. P. Monteiro, UNIFESP, were maintained in F12 medium (Invitrogen) supplemented with 10% FBS and streptomycin (0.1 g/ml)/penicillin (0.06 g/ml). The immortalized nontumorigenic mouse melanocyte cell line Melan A was maintained in RPMI 1640, pH 6.9, supplemented with 10% FCS and 200 nM phorbol 12-myristate 13-acetate (Sigma-Aldrich). They were tested with the peptide in culture without phorbol 12-myristate 13-acetate. All cell lines were cultured at 37 °C, under humid atmosphere and 5% CO_2.

Cell Viability Assay—Human tumor cell lines (10^4/well) or B16F10-Nex2 (5×10^3/well) cells were cultivated in 96-well plates under normal conditions. Cells were incubated with C7H2 peptide at different concentrations: 0.05, 0.1, 0.25, 0.5, 0.7, 0.8, and 1 mM. After 20 h of incubation at 37 °C, cells were collected with trypsin and counted in a Neubauer chamber using trypan blue exclusion test. All experiments were performed in triplicate, and the results are expressed as total number of cells in each well.

Peptides—Peptides were synthesized by the solid phase and classic solution methods at the Department of Biophysics of UNIFESP as described previously (16). Alternatively, peptides were purchased from Peptide 2.0 (Chantilly, VA). A stock solution of 1 mM was prepared by diluting the peptide C7H2 (YISCYNGATSYNQKFK) amidated at the C terminus or the scrambled control peptide (QYKISCNKYTGSFNYA) in 2% dimethyl sulfoxide and RPMI 1640 medium with 20% water.

Confocal Microscopy—B16F10-Nex2 cells (1×10^4) were distributed on round glass coverslips and incubated for 24 h at normal cell growth conditions. Cells were incubated for 1 h with 0.1 mM biotinylated C7H2, washed three times with PBS, and fixed with 3.7% paraformaldehyde for 30 min. Cells were then permeabilized in 0.1% Triton X-100 for 30 min followed by blocking for 1 h with 150 mM NaCl, 50 mM Tris, and 0.25% BSA, all from Sigma-Aldrich. After washing in PBS, cells were incubated for 1 h in the dark at 4 °C with streptavidin-FITC conjugate (Invitrogen) diluted 1:250 in PBS. Cells were then washed and stained with phalloidin-rhodamine (1:1,000) (Invitrogen) for 1 h (see Fig. 1*A*) or with deoxyribonuclease I-Alexa Fluor 594 conjugate (27 μg/ml) (Invitrogen) for 1 h (see Fig. 1*B*) followed by 10 μg/ml DAPI (Invitrogen) staining for 10 min. The coverslips were mounted on slides with 4 μl of Vectashield (Sigma) and observed in a Confocal Leica SP5 microscope, with a 63 × 1.4 oil objective; the Z series was obtained according with sampling criteria built in the software. DAPI, which stains the nucleus in blue, was examined at 350-nm excitation and 470-nm emission, and the streptavidin-FITC at 488-nm excitation and 525-nm emission. For phalloidin-rhodamine and deoxyribonuclease I-Alexa Fluor which stain, respectively, filamentous actin (F-actin) and globular actin (G-actin) in red, the excitation/emission at 540/565 nm and at 590/617 nm were used. Images were processed with ImageJ.

Peptide Effects on Polymerization and Depolymerization of Actin—Actin polymerization and depolymerization were measured using the Actin Polymerization Biochem kit (Cytoskeleton, Denver, CO) following the manufacturer's instructions. Briefly, 0.4 mg/ml (1:10 pyrene-labeled) monomeric actin was incubated on ice for 1 h in presence of ATP. A volume of 180 μl was pipetted on a black 96-well plate and read in a fluorometer every 60 s for 3 min to establish the fluorescent base line. The C7H2 peptide or a scramble peptide was added at 200 μM in 20 μl. After short incubation, samples were read at an excitation wavelength of 355 nm and emission wavelength of 410 nm in a fluorometer (SpectraMax-M2, Molecular Devices Software Pro 5.4, Sunnyvale, CA). After 30 min, the actin polymerization buffer (50 mM KCl, 2 mM $MgCl_2$, and 1 mM ATP) was added and the fluorescence read for 1 h. For depolymerization, a filamentous actin (F-actin) stock, 1 mg/ml (1:10 pyrene-labeled) was prepared with monomeric actin by adding 10 μl of 10× actin polymerization buffer in the presence of ATP and incubation at room temperature for 1 h. The F-actin is stable for 1 h after preparation. After 1 h, the F-actin stock was diluted to 0.2 mg/ml with G-buffer and 200 μl added to a 96-well plate. The C7H2 peptide or the scramble peptide was added at 200 μM, and the fluorescence at 410 nm in kinetic mode was measured for 1 h, as indicated above. The negative control had only the G-buffer. Depolymerization of F-actin was measured by reduction of fluorescence over time.

Mass Spectrometry—B16F10-Nex2 cells (4×10^7) were lysed using a buffer containing 1% Triton X-100, 10 mM Tris-HCl, 5 mM EDTA, 50 mM NaCl, 200 mM oxidized glutathione, pH 7.6, and a mixture of protease inhibitors (Pierce). The sample was incubated overnight at 4 °C with biotinylated C7H2. The reaction product was passed through a column of streptavidin-agarose (Pierce) and eluted with 2% urea. The eluate was separated in 10% SDS-PAGE, and the single band detected with colloidal Coomassie Blue was sliced and digested with trypsin (Promega) as described elsewhere (20).

An aliquot of the digested protein (4.5 μl) was injected in the analytic column C18 1.7-μm BEH 130 (100 μm × 100 mm) RP-UPLC (nanoAcquity UPLC; Waters) coupled to a Q-TOF Ultima API mass spectrometer (Micro Mass Waters) at a flow rate of 600 nl/min. A trapping column Symmetry C18 (180 μm × 20 mm) was used for sample desalting at a flow rate of 20 μl/min over 1 min. The gradient was 0–50% acetonitrile in 0.1% formic acid over 45 min. The instrument was operated in MS positive mode, data continuum acquisition from m/z 100 to 2,000 Da at a scan rate of 1 s and an interscan delay of 0.1 s. Data base searches for peptide identification from LC MS/MS experiments were done with Mascot Distiller v.2.3.2.0, 2009 (Matrix Science, Boston, MA) using carbamidomethyl-cys as fixed modification (monoisotopic mass 57.0215 Da), methionine oxidation as variable modification (monoisotopic mass 15.9949), and 0.1 Da MS and MS/MS fragment size tolerance.

Chemiluminescence-ELISA—A 96-well opaque plate (Nunc, Roskilde, Denmark) was coated with 0.5 mg/ml C7H2 diluted in carbonate-bicarbonate buffer, pH 9.2. The plate was washed with 0.05% Tween 20-PBS (T-PBS) and blocked overnight at 4 °C with 1% BSA. β-Actin (Cytoskeleton) was added at 5 μg/μl following a 1-h incubation. Anti-β-actin antibody (Novus Biologicals, Littleton, CO), at 1:1,000, was then added for 4 h. After incubation, the plate was washed extensively with T-PBS, and the secondary biotinylated 1:1,000 anti-mouse IgG (Sigma-Aldrich) and 1:1,000 streptavidin-peroxidase (Sigma-Aldrich) were added. The plate was washed 10 times with PBS, and the reaction was evaluated by chemoluminescence using ECL (1:1,000; Millipore) in a luminometer (SpectraMax) at 470 nm.

Chromatin Condensation—10^4 tumor cells, cultivated overnight on round glass coverslips, were treated with 0.3 mM C7H2 for 2 or 20 h, washed with PBS, and fixed for 30 min at room temperature with 2% formaldehyde. The cells were washed with PBS and stained with 2 μM Hoechst 33342 (Invitrogen) for 10 min. Cells were visualized in an Olympus BX-51 fluorescence microscope with immersion oil at 60× magnification. Images were processed with ImageJ. Apoptotic cells were detected by chromatin condensation and DNA leakage into the cytoplasm of tumor cells.

Nuclear Lamin Disintegration—10^4 tumor cells were cultivated in round glass coverslips and treated with 0.3 mM C7H2 for 1, 2, or 3 h at 37 °C. Cells were fixed with 2% formaldehyde for 1 h. They were then incubated with 1:5 anti-lamin B1 + B2 (Abcam) for 1 h, with the secondary biotinylated anti-mouse IgG 1:500 for 1 h, and were finally stained with streptavidin-FITC conjugate, 1:250. DAPI at 10 μg/ml was added to stain the nuclei at room temperature for 1 h. Cells were visualized with a 100× oil immersion objective (1.41 numerical aperture) in an Olympus BX61 microscope. Images were acquired using cell M^ software and processed by Blind 3D deconvolution using the software Auto Quant X2 and Adobe Photoshop CS4.

Caspase Activity—The activities of caspases 3, 6, 8, and 9 were measured by the ApoTarget Caspase Sampler kit (Invitrogen), according to manufacturer's instructions. Briefly, B16F10-Nex2 cells at 90% confluence were treated with 0.3 mM C7H2 peptide for 40 min at 37 °C. Next, cells were pelleted and resuspended in 50 μl of chilled Cell Lysis Buffer (Invitrogen) and incubated on ice for 10 min. After pelleting the cells for 1 min at 10,000 × g, the supernatant was recovered and transferred to a fresh tube. The protein concentration was determined by the Bradford method. The extract was diluted to 4 mg/ml protein in the Cell Lysis Buffer. An equal volume (50 μl) of 10 mM DTT diluted in the Reaction Buffer was added to each sample. The samples were incubated with 200 μM substrate, DEVD-pNA (caspase 3), VEID-pNA (caspase 6), IETD-pNA (caspase 8), and LEHD-pNA (caspase 9), at 37 °C for 2 h in a 96-well plate. Reactions were read at 400 nm in a microplate reader (SpectraMax-M2 software).

Cell Migration—The effect of peptide C7H2 on tumor cell migration was determined with 3×10^5 B16F10-Nex2 cells on 12-well plates. After cell adhesion, the peptide was added at 0.13 mM. After 12 h, vertical wounds were done across the wells using a 1,000-ml tip. Images were taken at 0, 3, 6, and 24 h after wounding. Cell migration was calculated by subtracting the average distance between the cell front at 0 h and that after 3, 6, or 24 h.

DNA Fragmentation—Cells (10^5/well) were cultivated in a 12-well plate and incubated for 20 h at 37 °C with either 0.3 mM C7H2 or control peptide at same concentration. After harvest-

ing the cells with PBS-EDTA (PBS and 0.02% EDTA), the DNA was extracted and analyzed as described previously (10).

Superoxide Anion Measurement—Superoxide anion production was measured by dihydroethidium (DHE) assay according to the manufacturer's instructions (Invitrogen). Briefly, 10^4 cells were cultivated on round glass coverslips and treated with 0.3 mM C7H2 for 1, 2, or 3 h at 37 °C. Treated cells were then incubated with 5 μM DHE at room temperature for 30 min. The conversion of DHE to ethidium by oxidation was detected by fluorescence microscopy in an Olympus BX-51 microscope using a 60× oil immersion objective. Images were processed with ImageJ. As a positive control, cells were treated with 5 mM H_2O_2 at 37 °C for 20 min.

Transmission Electron Microscopy—B16F10-Nex2 cells (5×10^4) were cultivated on plastic disks made from Aclar film. Cells were then incubated with 0.3 mM C7H2 for 2 h at 37 °C and fixed in a solution of 2.5% glutaraldehyde and 2% formaldehyde in 0.1 M sodium cacodylate buffer, pH 7.2, at room temperature for 20 h. Next, cells were washed in the same buffer for 10 min, fixed with 1% osmium tetroxide in 0.1 M cacodylate at pH 7.2 for 30 min, and washed with water for 10 min at room temperature. Subsequently, cells were treated with an aqueous solution of 0.4% uranyl acetate for 30 min and washed with water for 10 min. After fixation, cells were dehydrated in graded ethanol (70, 90, and 100%), treated quickly with propylene oxide, and embedded in EPON. Semi-thin sections from selected regions were collected on grids and stained in alcoholic 1% uranyl acetate and in lead citrate prior to examination in a Jeol 1200 EXII electron microscope (Tokyo, Japan).

TUNEL Assay—TUNEL was performed according to the manufacturer's instructions (In Situ Cell Death Detection kit, Fluorescein; Roche Applied Science). Briefly, 1×10^4 cells were cultivated in round glass coverslips and treated for 2 h with 0.3 mM C7H2 peptide. Cells were fixed in 2% formaldehyde for 30 min at room temperature. They were then permeabilized with 0.1% Triton X-100 for 30 min at room temperature and incubated with TUNEL in the reaction buffer with dUTP-fluorescein at 37 °C for 1 h, then stained with 10 μg/ml DAPI for 10 min, and visualized in a Bio-Rad 1024UV instrument coupled to a Zeiss Axiovert 100 microscope using a 63×1.4 NA differential interference contrast (or 100×1.4 NA phase contrast) oil immersion lenses. Images were processed with ImageJ. As a positive control, cells were treated with 1 μg/ml actinomycin D (Sigma-Aldrich) for 1 h.

Phosphatidylserine Translocation—Tumor cells (5×10^5) were cultivated in 6-well plates with 0.3 mM C7H2 peptide or without peptide for 12 h at 37 °C and 5% CO_2. Treated and untreated cells (1×10^6) were harvested with trypsin and were incubated with binding buffer (10 mM HEPES/NaOH, pH 7.5, 140 mM NaCl, and 2.5 mM $CaCl_2$) in the presence of propidium iodide and annexin V (Annexin V-FITC Apoptosis Detection kit; Sigma) for 10 min at room temperature and analyzed by flow cytometry (Becton-Dickinson FACSCalibur apparatus) with CellQuest software.

Animals and Experimental Lung Metastasis—All animal experiments were carried out using protocols approved by the Ethics Committee for animal experimentation of Federal University of São Paulo, Brazil. Male C57BL/6 7–8-week-old mice were challenged intravenously with 5×10^5 syngeneic B16F10-Nex2 melanoma cells/mouse (0.1 ml). For protection experiments five groups of five animals received on days 1, 3, 5, 7, 9, 11 after tumor cell challenge, intraperitoneal doses of 300 μg of C7H2, or Y1A, I2A, S3A, and C4A substituted peptides using the same protocol. After 20 days, lungs were collected from animals of each group and inspected for metastatic colonization.

Statistical Analysis—Significant differences were assessed using Student's *t* test with *p* values <0.05.

RESULTS

C7H2 Affects Cytoskeleton by Binding to β-Actin in Tumor Cells—In the context of antitumor therapy and drug development, synthetic peptides synthesized based on CDRs may represent an endless source of potential therapeutic agents. In the last 5 years, we have identified and reported the antitumor, antiviral, and antimicrobial activity of several CDR-based peptides which is largely independent of the specificity of the native antibody. The synthetic peptide (C7H2) designed based on the V_H CDR2 of mAb C7 (21) significantly reduced B16F10 melanoma growth and lung colony formation by triggering tumor apoptosis. However, the receptor of C7H2 as well as the mechanism by which C7H2 induces apoptosis in tumor cells remained unclear. Initially, we sought therefore to determine the molecular target of the C7H2 peptide.

Using confocal microscopy we examined the distribution of C7H2 peptide in the tumor cells. To that end, B16F10-Nex2 cells were incubated with biotinylated-C7H2 for 1 h then were fixed and permeabilized, followed by incubation with streptavidin-FITC. Interestingly, an intense and remarkable localization of C7H2 peptide was observed mainly at the cell surface but also in the cytosol, seemingly along the cytoskeleton fibers (Fig. 1*Ab*). A closer analysis revealed that C7H2 co-localized with phalloidin-rhodamine, a well characterized toxin known to bind F-actin (Fig. 1*Ad*). Binding of C7H2 to G-actin was also shown by co-localization with DNase I (Fig. 1*Bd*), thus suggesting that C7H2 may bind and disturb the cytoskeleton dynamics therefore leading the cells to apoptosis.

There is compelling evidence suggesting that alterations in the cytoskeleton dynamics, involving actin polymerization or late depolymerization, and ROS production, is sufficient to trigger apoptosis in a variety of cell types (22). To address the possibility of C7H2 promoting the polymerization of actin, monomeric pyrene-labeled actin (pyrene G-actin) was incubated with 200 μM C7H2 peptide, scrambled control peptide, or with ATP-containing polymerization buffer (positive control). As depicted in Fig. 1*C*, the polymerization of G-actin was observed in a time-dependent manner after addition of C7H2 peptide reaching its maximum after 30 min, whereas the C7H2 scrambled peptide (negative control) did not show any significant activity on actin polymerization, suggesting that actin is the molecular target of C7H2 in tumor cells. Moreover, spontaneous depolymerization of F-actin was hindered by C7H2 but not by the scramble peptide for at least 1 h, suggesting that C7H2 not only promotes polymerization of monomeric actin but also plays a role in F-actin stabilization (Fig. 1*D*).

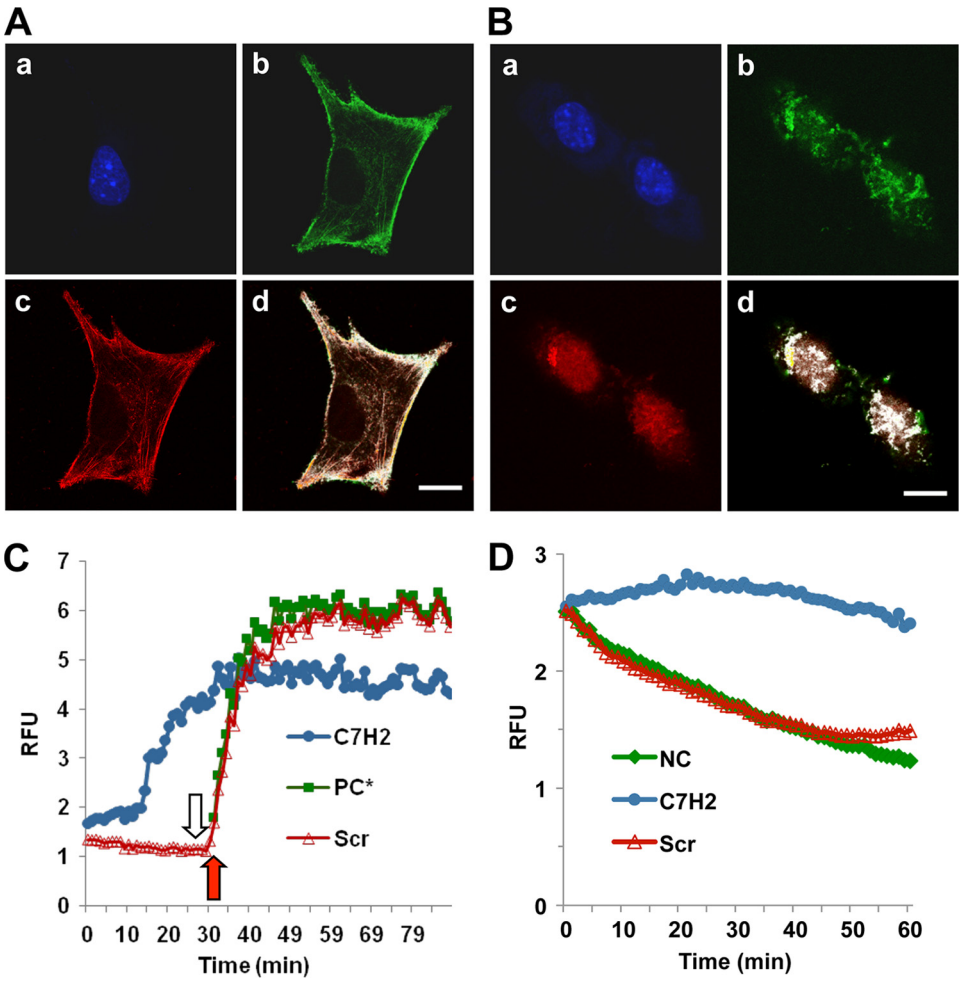

FIGURE 1. **Binding of C7H2 to actin cytoskeleton and actin polymerization.** *A*, co-localization of phalloidin and C7H2 in melanoma cells. B16F10-Nex2 tumor cells were treated with biotinylated C7H2, fixed with paraformaldehyde, and permeabilized with Triton X-100. Cells were stained with DAPI (*a*), streptavidin-FITC (*b*), and phalloidin-rhodamine (*c*) and were examined by confocal microscopy; *d*, merge, showing co-localization. *Scale bar*, 20 μm. *B*, co-localization of DNase I and C7H2 in melanoma cells. B16F10-Nex2 tumor cells were treated with biotinylated C7H2, fixed, and permeabilized as in *A*. Cells were stained with DAPI (*a*), streptavidin-FITC (*b*), and DNase I-Alexa Fluor 594 (*c*) and were examined by confocal microscopy; *d*, merge, showing co-localization. *Scale bar*, 20 μm. *C*, pyrene G-actin (0.4 mg/ml) added to a 96-well plate. C7H2 at 200 μM (●, *blue*) and the scramble peptide Scr-C7H2 (△, *red*) were added, and the fluorescence at 410 nm was measured in kinetic mode. At the end of 30 min (*open arrow*) or at the same time without previous incubation with peptide (*red arrow*), the ATP-containing polymerization buffer was added as a positive control (*PC*, green*). *D*, pyrene F-actin from stock incubated for 1 h diluted to 0.2 mg/ml and added to a 96-well plate. C7H2 at 200 μM (●, *blue*) and the scramble peptide Scr-C7H2 (△, *red*) were added, and the fluorescence at 410 nm in kinetic mode was measured. Negative control, *NC* (◆, *green*), incubation with the G-buffer.

To identify further the molecular target of C7H2, biotinylated C7H2 peptide was incubated with B16F10-Nex2 cell lysate, and the complex peptide-receptor was isolated by affinity chromatography in a streptavidin-agarose column. The purified complex was resolved in 10% SDS-PAGE showing a single band of 43 kDa detected with colloidal Coomassie Blue. After recovering the sample, the complex was digested with trypsin-generating fragments that were analyzed by Q-TOF mass spectrometry. Eight peptide sequences (hits) were identified which identified β-actin (ACTB_MOUSE, accession P60710.1 GI 46397334; ACTB_HUMAN, accession P60709.1 GI 46397333) as the main receptor of C7H2 in tumor cells (Fig. 2*A*).

Finally, the interaction of C7H2 and β-actin was validated based on a modified chemiluminescent ELISA. The C7H2 peptide was directly immobilized on the plate, and after blocking, and extensive washes, the recombinant β-actin was added. Next, anti-β-actin antibody was added to the plate followed by incubation with the chemiluminescent substrate, as described under "Experimental Procedures." As depicted in Fig. 2*B*, addition of the recombinant β-actin on C7H2-coated plate increased 3.1-fold the binding of anti-actin antibody compared with β-actin and antibody alone ($p < 0.01$).

The immediate effect involving actin interaction would be interference with cell migration, which depends on actin dynamics. C7H2 peptide at low concentration clearly inhibited tumor cell migration using a "wound" assay (Fig. 2*C*). Altogether, these data suggested that, subsequent to C7H2 binding to β-actin, significant alterations on the cytoskeleton dynamics of tumor cells could lead them to apoptosis.

Caspase 3, Caspase 8, and Anion Superoxide Are Triggered during Apoptosis Induced by C7H2—We have shown previously that the C7H2 peptide caused DNA fragmentation in murine and human melanoma cell lines whereas its scrambled form was inactive. Moreover, we had evidence that the apoptosis triggered by C7H2 was in fact caspase-dependent

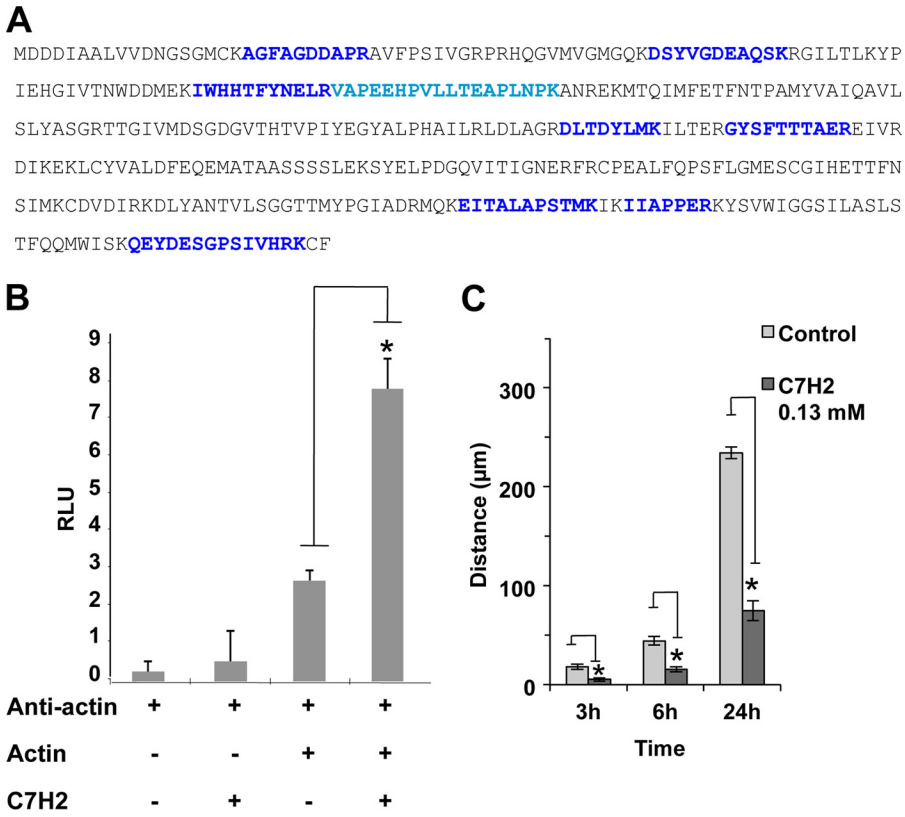

FIGURE 2. **Binding of C7H2 to β-actin and inhibition of cell migration.** *A*, B16F10-Nex2 cell lysate was incubated with biotinylated C7H2. Proteins were separated in streptavidin-agarose and eluted with urea. The eluate was separated in SDS-PAGE, and the single band detected was analyzed by mass spectrometry. Peptides from LC MS/MS leading to β-actin identification are shown, over the entire sequence, in *blue*. *B*, ELISA plates were coated with BSA with or without peptide C7H2 at 500 μg/ml. β-Actin was added followed by anti-actin antibody and the secondary anti-IgG. A clear binding of β-actin to C7H2 is demonstrated. $p < 0.01$. *C*, cells adhering to 12-well plates were treated with 0.13 mM C7H2. After 12 h, wounds across the wells were done, and cell migration was scored at different times. *Error bars*, S.D.

once apoptosis was inhibited by Z-VAD, a pan-caspase inhibitor (10).

To establish further an apoptosis mechanism triggered by C7H2 in clinically relevant tumor cells, the highly invasive and metastatic human melanoma cell line A2058 was incubated with 0.3 mM C7H2 for 20 h at 37 °C. A2058 cells were then stained by the DNA dye Hoechst 33342 and visualized under fluorescence microscopy. As observed in Fig. 3*A*, incubation with C7H2 induced a remarkable chromatin condensation in A2058 cells (Fig. 3*Ac*) compared with untreated cells (Fig. 3*A*, *a* and *b*). Similar *in vitro* results were also observed when the C7H2 peptide was added, in U87-MG, SKBr3, HeLa, and HCT cell lines. The frequency of cells with condensed chromatin in the various tumor cell lines was the following: A2058, 43%; U87-MG, 19%; SKBR3, 29%; HCT-8, 26%; and HeLa cells, 45%.

Additionally, an intense DNA staining pattern was observed in the cytoplasm, suggesting the disruption of the nuclear membrane. This result was later confirmed by deconvolution microscopy of the nuclear lamina framework of B16F10-Nex2 cells incubated with 0.3 mM C7H2 for up to 3 h (Fig. 3*B*). The same effect was observed in HeLa cells (supplemental Fig. S1), again showing that with few differences in time and intensity murine melanoma and human tumor cells responded similarly to the apoptotic C7H2 peptide.

Because the proteolysis of lamins is often observed in different cells undergoing apoptosis due to increase of caspase activity (23), we have assessed the caspase activity profile in B16F10-Nex2 cells after treatment with the C7H2 peptide. To that end, melanoma cells were incubated with 0.3 mM C7H2 peptide for 40 min under normal growth conditions. As shown in Fig. 3*C*, the activity of caspase 3 and 8 was significantly higher (by 1.8- and 2-fold, respectively) on treated cells compared with untreated samples (*CTL*). The increased activation of caspases 8 and 3 and not of caspase 9 might indicate a direct pathway triggered by ROS as discussed below. Interestingly, no significant increase of caspase 6 activity was detected after C7H2 treatment most likely because caspase 6 is activated at later stages of the apoptosis cascade, cleaving lamin A, whereas caspase 3 is activated at the early phases of apoptosis, and it is known to cleave lamin B prior to DNA fragmentation. In fact, a significant DNA fragmentation "ladder" pattern at ~200-bp intervals was also observed when A2058 cells were treated with 0.3 mM C7H2 peptide for 20 h (Fig. 3*D*). Similar results were also found in HeLa, U87-MG, and SKBR3 cell lines (supplemental Fig. S2).

Finally, because concomitant increase of caspase-8 activity and anion superoxide production during apoptosis has been documented (24), as we also observed in HeLa cells (supplemental Fig. S3), we measured the production of O_2^- in B16F10-Nex2 cells treated with the C7H2 peptide. Tumor cells were treated with C7H2 (0.3 mM) for 1–3 h, and the anion superoxide production was detected by DHE. As shown in Fig. 3*E*, the pro-

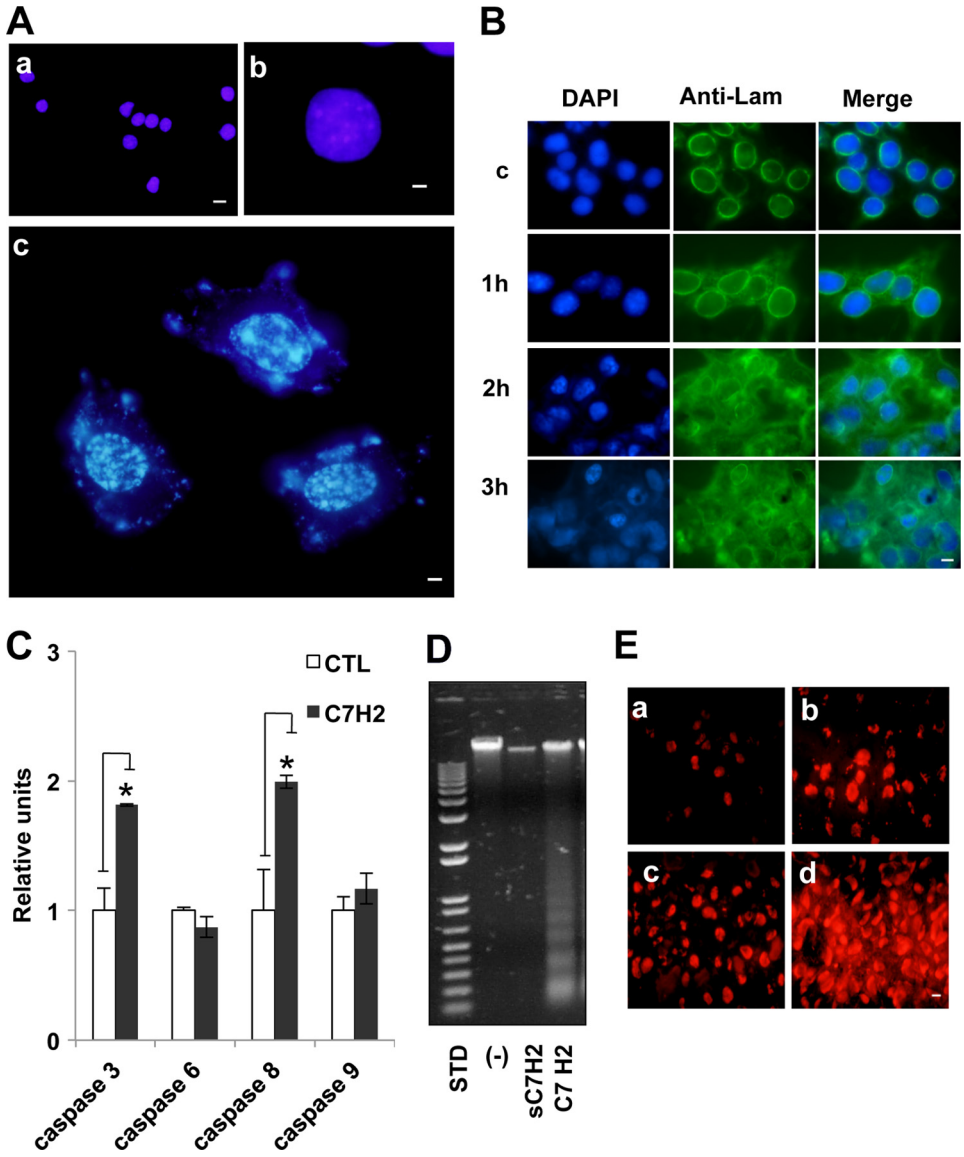

FIGURE 3. **C7H2 induces nuclear and mitochondrial alterations.** *A*, chromatin condensation seen by Hoechst 33342 staining of A2058 human melanoma cells treated with C7H2 at 0.3 mM for 20 h. Nucleic acid leakage into the cytoplasm is also seen. *a* (*scale bar*, 20 μm) and *b* (*scale bar*, 80 μm), control cells; *c* (*scale bar*, 80 μm), treated cells. Cells were examined by fluorescence microscopy. *B*, early disintegration of nuclear lamin following 0.3 mM C7H2 treatment of B16F10-Nex2 cells at the indicated times. *First column*, DAPI nuclear staining; *middle column*, anti-lamin B1 + B2 antibody, secondary biotinylated anti-mouse IgG and streptavidin-FITC conjugate; *third column*, merge. Deconvolution microscopy, *scale bar*, 20 μm. *C*, B16F10-Nex2 melanoma cells incubated with C7H2 for 40 min induced increased production of caspases 3 and 8 analyzed by colorimetric assay ($p < 0.01$) but not caspases 6 and 9. *D*, DNA degradation in A2058 melanoma cells, induced by C7H2 at 0.3 mM for 20 h; a control with scramble peptide is shown and also the standard (*STD*) DNA ladder pattern fragments. *E*, abundant anion superoxide produced by B16F10-Nex2 cells treated with 0.3 mM C7H2. *a*, untreated cells; *b*, positive control with 5 mM H_2O_2; *c* and *d*, time-dependent anion superoxide production detected with DHE. *Scale bar*, 20 μm.

duction of anion superoxide is dramatically increased with time (Fig. 3*E*, *c* and *d*, 1 h and 3 h, respectively) surpassing that formed on tumor cells treated with 5 mM H_2O_2 (Fig. 3*Eb*). The same increased production of anion superoxide was seen in peptide-treated HeLa cells (supplemental Fig. S3).

Ultrastructural and Apoptotic Effects of C7H2—Alternatively, to study the cellular phenotypic alterations induced by C7H2 peptide, B16F10-Nex2 cells were treated with 0.3 mM C7H2 for 2 h and observed under electron microscopy (Fig. 4*A*). Significant alterations included detachment of the nuclear membrane, peripheral accumulation of chromatin, chromatin condensation, and disintegration of cytoplasmic structures including mitochondria disintegration and formation of vesicles in the cytoplasm. Along with this experiment, A2058 cells were treated for either 2 h or 12 h with 0.3 mM C7H2, and apoptosis was detected by classical well established methods, TUNEL assay (Fig. 4*Bc*), and flow cytometry (Fig. 4*C*), respectively. Both experiments revealed that tumor cells went through apoptosis quickly after the addition of C7H2 (approximately after 2 h). Furthermore, the apoptotic process as observed by annexin V cell staining (treated cells, 28.7%; untreated, 8.9%) was accompanied by aptonecrosis as observed by propidium iodide and annexin V cell staining (treated cells, 37.8%; necrotic; nontreated, 16.25%). Likewise, other human tumor cell lines (U87-MG, HCT-8, and Siha), displayed similar susceptibility to C7H2 treatment after 12 h, showing variable

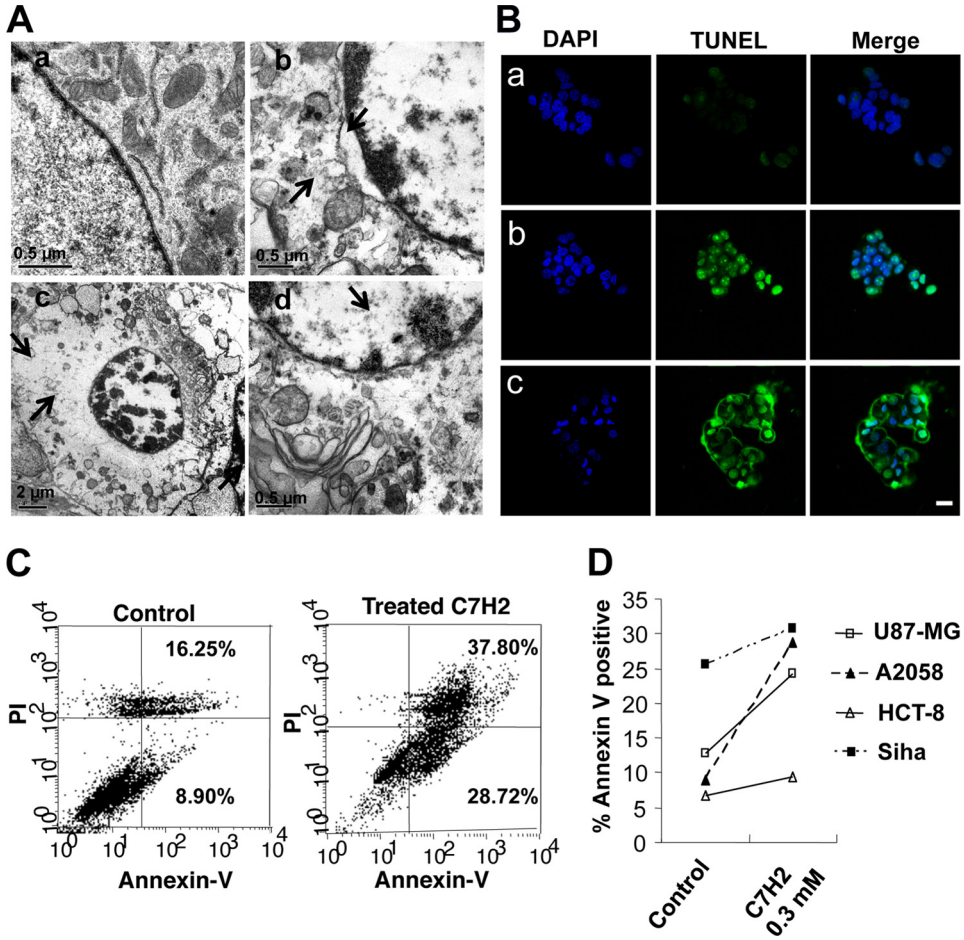

FIGURE 4. **TUNEL assay and morphological alterations induced by C7H2.** *A*, transmission electron microscopy of B16F10-Nex2 cells treated with 0.3 mM C7H2 for 2 h. *a*, control untreated cell; *b*, peptide-treated cell with detached nuclear membrane, peripheral accumulation of chromatin and altered cytoplasm, swollen and disrupted organelles (*arrows*); *c* and *d*, cells with condensed chromatin and major disintegration of cytoplasmic structures including mitochondria (*arrows*). *B*, TUNEL assay in confocal microscopy, showing untreated cells (*a*), positive control with 1 μg/ml actinomycin-treated cells (*b*), and 0.3 mM C7H2-treated A2058 melanoma cells for 2 h (*c*). *Scale bar*, 20 μm; *C*, annexin V binding in A2058 melanoma cells treated with 0.3 mM C7H2 for 12 h. propidium iodide labeling is also shown. *D*, annexin V binding of four different human cancer cells treated with C7H2 for 12 h. Cells were analyzed by FACS.

increases of annexin V binding: treated cells/nontreated U87-MG 1.91; HCT-8, 1.38; Siha, 1.22 (Fig. 4*D*). U87-MG, SKBr3, HCT-8, and HeLa cell lines also showed similar staining pattern when tested by TUNEL assay (supplemental Fig. S4).

Overall, these results suggest that the rapid apoptosis signal induced by C7H2 bound to β-actin in tumor cells simultaneously produces hydrolytic enzymes, caspases, nucleases, and accumulation of anion superoxide. The increased levels of O_2^- also interfere with the cell cytoskeleton dynamics, therefore potentializing the C7H2 cytotoxic activity.

C7H2 Displays Cytotoxic Activity toward Several Human Tumor Cell Lines in Vitro—To address the use of C7H2 as a potential therapeutic anticancer agent, we have tested the cytotoxic activity of C7H2 *in vitro* toward several human tumor cell lines, including breast, colon, uterine cervix cancer, glioblastoma, and melanoma for up to 20 h at normal growth conditions (Table 1). The narrow range of mean variability observed in Table 1 suggests that all different tumor cell lines are significantly and similarly sensitive to C7H2. This statement was further confirmed by *in vitro* analyses as described above and in the supplemental material.

TABLE 1
***In vitro* C7H2 cytotoxicity in human tumor cell lines**

Cell lines	Cancer type	EC_{50}
		mol/liter × 10^{-3}
A2058	Melanoma	0.22 ± 0.028
HCT-8	Colon	0.33 ± 0.032
LS180	Colon	0.15 ± 0.025
MCF7	Breast	0.22 ± 0.023
MDA	Breast	0.17 ± 0.042
SKBR3	Breast	0.20 ± 0.019
U87MG	Glioblastoma	0.19 ± 0.019
SiHa	Uterine cervix	0.47 ± 0.082
HeLa	Uterine cervix	0.18 ± 0.074

The C7H2 cytotoxic activity toward nontumorigenic cell lines (rabbit aortic endothelial cells, mouse embryonic fibroblasts, GM637, and Melan A) was also evaluated *in vitro*. Surprisingly, these nontumorigenic cell lines were not sensitive to C7H2 treatment, nor did they show any significant cellular alterations under the same conditions described above. The percentages of live cells counted by trypan blue exclusion staining after treatment with C7H2 were as follows: rabbit aortic endothelial cells, 91 ± 2.2%; mouse embryonic fibroblasts; 88.3 ± 5.7%; GM637 cells, 94.2 ± 2.1%. Alternatively, the Melan A cell line was incubated with 0.3 mM C7H2 for 3 h under

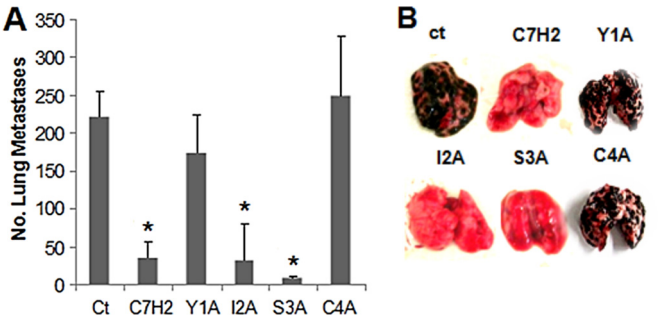

FIGURE 5. **Antimetastatic effects of peptides.** Lung colonization of B16F10-Nex2 cells in a syngeneic system was used to test the protective activity of C7H2 and N-terminal alanine-substituted analogs Y1A, I2A, S3A, or C4A. Protective activity of peptides injected intraperitoneally with doses of 300 μg using the protocol indicated under "Experimental Procedures" is shown. Mice ($n = 5$/group) were challenged with 5×10^5 syngeneic B16F10-Nex2 melanoma cells (0.1 ml/mouse). *, $p < 0.01$; *error bars*, S.D.

normal growth conditions. After incubation, 83.3% viable Melan A cells were counted by trypan blue. Further incubation of Melan A cells for up to 21 h in fresh growth medium rendered 87.2% live cells. However, Melan A as well as the other nontumorigenic cells were significantly inhibited by 95% after 24-h incubation in presence of 0.3 mM C7H2.

To study further the possible toxicity exerted by C7H2 to normal tissue, C57BL/6 mice (6–8 weeks old) weighing from 22 to 25 g, were injected for 3 consecutive days with a dose of 25 mg/kg per mouse of C7H2. After 2 days of the last dose, animals were sacrificed, and the organs such as liver, brain, kidneys, spleen, and intestine were examined for any sign of toxicity. No significant histopathological alterations were observed under this condition (data not shown), therefore indicating that C7H2 could be a suitable peptide for treatment of several kinds of cancer in humans.

N-terminal Sequence of C7H2 Is Essential to Maintain Its Tumor Cytotoxic Activity in Vivo—Previously (10), we have suggested that the C-terminal sequence of C7H2 could play a role in the peptide binding to a cell surface receptor because it competed with the whole peptide reducing its cytotoxicity, without itself being cytotoxic. Although the C-terminal peptide seems to compete for β-actin binding *in vitro*, such a fragment is not able to induce β-actin polymerization (data not shown) here established as an important step for C7H2 cytotoxic activity. Nonetheless, the peptide fragment synthesized based on the N-terminal region of C7H2 was demonstrated to be essential for the C7H2 peptide activity *in vivo*.

Using the syngeneic murine melanoma model of B16F10-Nex2 cells, we showed that substitution of tyrosine with alanine (Y1A) and cysteine with alanine (C4A) resulted in a significant lack of protection revealed by the increased number of lung metastases in mice treated with the modified peptide compared with unmodified peptide (Y1A, 150; C4A, 250; C7H2, 45) (Fig. 5). Altogether, this result shows that, at least *in vivo*, the specificity and antitumor activity of the C7H2 peptide rely on the N-terminal region rather than the C-terminal region. Using the same peptide-coated ELISA, we observed that compared with C7H2, the C4A bound poorly to β-actin (supplemental Fig. S5), but its lack of protective activity *in vivo* may involve other factors that are presently being investigated.

DISCUSSION

The diversity of peptides and their specific binding to cellular targets place them in a potential new class of drugs to be used in cancer therapy in addition to small molecules. Synthetic functional peptides, phage-derived and a number of cyclic and linear peptides from natural sources, have been investigated for antitumor activities. Exotic plants, venoms and toxins, insects, fish, a marine molusc, are among the natural products looked for peptides, aiming at a great diversity of molecular sequences that could be useful in cancer therapy (25–29). The potential of natural anticancer apoptotic/necrotic, function-blocking, antiangiogenic, and immunostimulatory peptides to induce tumor regression has been reviewed by Bhutia and Maiti (1). The unexpected introduction of immunoglobulins in this scenario as a source of bioactive peptide sequences independent of antibody specificity (10, 12) provides in perspective another depository of molecular species that can be tested for antiinfective and antitumor activities. If only considering the CDRs, at least one or two CDRs per immunoglobulin molecule, tested as synthetic peptides, may be expected to exert antitumor cytotoxic activities, including growth arrest, inhibition of cell migration, cell signaling and metastasis, as well as apoptosis/necrosis, *in vitro* and *in vivo* (10, 16).

Different receptors and interfering pathways are expected for the CDRs because of the high diversity of their amino acid sequences. Here, we investigated CDR peptide C7H2, which is apoptotic in a variety of cancer cells, both murine and human. The EC_{50} values *in vitro* are in the same range for this peptide, suggesting that a conserved target is involved. Apoptosis-inducing peptides aiming at cancer therapy have been investigated which target members of the apoptosis signaling pathway. They are originated from Bak, Bax, Bad, Bim, Smac, and also from survivin and p53 (30). Others, however, display quite different activities and recognize different targets. In the case of C7H2, the target has been identified as β-actin, which agrees with the broad antitumor activity of the peptide toward many different cancer cells.

G-actin polymerizes to form F-actin with the concomitant hydrolysis of ATP. It has been shown that apoptosis in HL-60 cells involves transient actin polymerization and late depolymerization (31) and that actin stabilization may enhance apoptosis (32). In both cases a relation exists between the actin cytoskeleton and transduction of intracellular signals leading to apoptosis.

Identification of β-actin as target of C7H2 was supported by the following methodologies: mass spectrometry of the cell-lysate ligand of biotinylated-C7H2; direct ELISA binding of β-actin to the peptide-coated surface; and confocal microscopy, which showed the co-localization of biotin-C7H2 with both phalloidin-rhodamine (F-actin) and DNase I (G-actin). Peptide binding to β-actin not necessarily is associated with cell apoptosis and probably in many cases is not. However, C7H2 was able to promote actin polymerization, which is not observed with the corresponding scramble peptide nor with its C-terminal fragment. The latter apparently plays a role in the peptide binding to the target cell (10). The induced polymerization leveled out a little below the maximum obtained with the

control salts and ATP, but it was sufficiently evident to suggest that the peptide can interfere in the G-actin pool increasing the conversion to F-actin. Furthermore, C7H2 peptide was able to hinder F-actin depolymerization for a considerable time, clearly suggesting interference in actin dynamics. A direct correlation exists between actin dynamics and mitochondria-dependent apoptosis. F-actin stabilization as by jasplakinolide in Jurkat T cells rapidly induces apoptosis followed by an increase in caspase 3 activation (23, 33). The same was observed with HL-60 cells (34), which are susceptible to C7H2 apoptotic effects (10). A model outlining links between actin dynamics and apoptotic signaling in animal cells was proposed by Frankin-Tong and Gourlay (35).

C7H2 peptide seemingly binds to β-actin in melanoma cells, and biotinylated C7H2 reacted with nonpermeabilized tumor cells in a way similar to anti-β-actin antibody (supplemental Fig. S6). The expression of cell surface actin has been shown in cancer cells (36) and in a few other cells, *e.g.* catecholaminergic cells that bind plasminogen (37), calf pulmonary artery endothelial cells in culture (38), and lymphocytes (39, 40).

We therefore compared the cytotoxicity of the peptide in both tumorigenic and nontumorigenic cells. *In vitro*, tumor cells and in particular melanoma cells, were killed by apoptosis after a 2–3-h exposure to 0.3 mM C7H2, although some earlier effects (*e.g.* chromatin condensation) could be seen. After 3 h of *in vitro* treatment, all four nontumorigenic cell lines including Melan A were unaffected by the same concentration of C7H2 that was apoptotic in tumor cells. Toxicity of the peptide was seen after 24 h in nontumorigenic cells in culture. Such toxicity *in vitro*, however, was not detected *in vivo* in healthy mice injected with very high doses of the peptide for 3 consecutive days and examined 2 days after. Clearly, the susceptibility to the peptide is much different in cancer cells compared with normal cells presumably because of the greater exposure of β-actin at the cell surface and of F-actin dynamics at the tumor cell extensions, faster internalization, and response to the peptide-induced apoptosis.

Alterations in murine and human tumor cells which are compatible with apoptosis are documented in the present work including chromatin condensation, DNA degradation (direct detection and TUNEL), annexin V binding (and partial propidium iodide staining), lamin disruption, caspase 3 and 8 activation, anion superoxide production and major destruction of cell organelles with cell rounding and shrinkage.

The various steps of C7H2 peptide activity can be suggested. The peptide can act on β-actin promoting its polymerization (as shown *in vitro*) and decreasing actin turnover. Changes to the dynamics of the actin cytoskeleton have been implicated in the release of ROS from mitochondria and subsequent cell death. In fact, accumulation of aggregates of F-actin triggers an increase of ROS in the cytosol (22). In early apoptosis there is an increased co-localization of F-actin and mitochondria (41) followed by translocation of cofilin, a key regulator of actin dynamics, which promotes depolymerization of actin filaments (42). Mitochondrial targeting of cofilin induces cytochrome *c* leakage and apoptosis (43). The regulation of actin pools through the action of actin-binding proteins, has been implicated in apoptosis regulation in both mammalian and yeast cells (44).

The C7H2 peptide induced the activation of caspase 8 and caspase 3. Because there is no evidence of the extrinsic apoptosis pathway or the simultaneous activation of caspase 9, it is possible that a caspase 8-Bid-Bax pathway can be triggered by ROS as in *N*,*N*-dimethyl phytosphingosine-treated leukemia cells (24). As shown in the present work, superoxide anions are abundantly produced in C7H2-treated cells. Caspase 8 acts upstream of caspase 3 and caspase 8 mediated the mitochondrial pathway in *N*,*N*-dimethyl phytosphingosine-induced apoptosis. As suggested, ROS are critical regulators of caspase 8-mediated apoptosis. Accordingly, in a study with pyrimethamine in metastatic melanoma, it was found that the drug, which generates ROS, induced upstream caspase activation (caspase 8), bypassing CD95/Fas engagement, similar to what had been previously observed by the same authors in activated lymphocytes from a patient with a lymphoproliferative syndrome (45).

We have suggested before (10) that the C-terminal sequence of C7H2 could play a role in the peptide binding to a cell surface receptor because it competed with the whole peptide reducing its cytotoxicity, without itself being cytotoxic. Alanine scanning also showed that C-terminal amino acids were important for peptide antitumor activity *in vitro*. However, the C-terminal peptide (Ct) did not induce β-actin polymerization as compared with the C7H2 peptide (data not shown). Presently, we focused on the N-terminal amino acids and their importance for C7H2 protective activity *in vivo*. Either tyrosine and cysteine residues, but not isoleucine or serine, were essential for C7H2 protective activity using the metastatic model of syngeneic B16F10-Nex2 melanoma. This result further confirms the specificity of the C7H2 peptide in its *in vivo* antitumor activity. *In vivo*, however, the mechanism of C7H2 antitumor protective activity may involve levels of complexity greater than those outlined *in vitro*. By targeting a common substrate, actin, that is expressed predominantly at the cell surface of cancer cells and abundantly at cell projections of invading tumor cells, the C7H2 peptide is a candidate to be developed as an anticancer drug.

Acknowledgments—We thank the Ludwig Institute for Cancer Research, São Paulo branch, Dr. O. Keith Okamoto, Dr. Hugo P. Monteiro, and Dr. Luiz F. L. Reis for the cell lines used in the present study. We thank Dr. Edna Haapalainen for the electron microscopy of melanoma cells.

REFERENCES

1. Bhutia, S. K., and Maiti, T. K. (2008) Targeting tumors with peptides from natural sources. *Trends Biotechnol.* **26,** 210–217
2. Daffre, S., Bulet, P., Spisni, A., Ehret-Sabatier, L., Rodrigues, E. G., and Travassos, L. R. (2008) in *Studies in Natural Products Chemistry* (Atta-ur-Rahman, ed) pp. 597–691, Elsevier, The Netherlands
3. Janin, Y. L. (2003) Peptides with anticancer use or potential. *Amino Acids* **25,** 1–40
4. Polonelli, L., Magliani, W., Conti, S., Bracci, L., Lozzi, L., Neri, P., Adriani, D., De Bernardis, F., and Cassone, A. (2003) Therapeutic activity of an engineered synthetic killer antiidiotypic antibody fragment against experimental mucosal and systemic candidiasis. *Infect. Immun.* **71,** 6205–6212
5. Magliani, W., Conti, S., Salati, A., Arseni, S., Ravanetti, L., Frazzi, R., and

Polonelli, L. (2004) Engineered killer mimotopes: new synthetic peptides for antimicrobial therapy. *Curr. Med. Chem.* **11,** 1793–1800
6. Cenci, E., Bistoni, F., Mencacci, A., Perito, S., Magliani, W., Conti, S., Polonelli, L., and Vecchiarelli, A. (2004) A synthetic peptide as a novel anticryptococcal agent. *Cell. Microbiol.* **6,** 953–961
7. Savoia, D., Scutera, S., Raimondo, S., Conti, S., Magliani, W., and Polonelli, L. (2006) Activity of an engineered synthetic killer peptide on *Leishmania major* and *Leishmania infantum* promastigotes. *Exp. Parasitol.* **113,** 186–192
8. Casoli, C., Pilotti, E., Perno, C. F., Balestra, E., Polverini, E., Cassone, A., Conti, S., Magliani, W., and Polonelli, L. (2006) A killer mimotope with therapeutic activity against AIDS-related opportunistic micro-organisms inhibits *ex vivo* HIV-1 replication. *AIDS* **20,** 975–980
9. Polonelli, L., Magliani, W., Ciociola, T., Giovati, L., and Conti, S. (2011) From *Pichia anomala* killer toxin through killer antibodies to killer peptides for a comprehensive anti-infective strategy. *Antonie Van Leeuwenhoek* **99,** 35–41
10. Polonelli, L., Pontón, J., Elguezabal, N., Moragues, M. D., Casoli, C., Pilotti, E., Ronzi, P., Dobroff, A. S., Rodrigues, E. G., Juliano, M. A., Maffei, D. L., Magliani, W., Conti, S., and Travassos, L. R. (2008) Antibody complementarity-determining regions (CDRs) can display differential antimicrobial, antiviral and antitumor activities. *PLoS One* **3,** e2371
11. Gabrielli, E., Pericolini, E., Cenci, E., Ortelli, F., Magliani, W., Ciociola, T., Bistoni, F., Conti, S., Vecchiarelli, A., and Polonelli, L. (2009) Antibody complementarity-determining regions (CDRs): a bridge between adaptive and innate immunity. *PLoS One* **4,** e8187
12. Magliani, W., Conti, S., Cunha, R. L., Travassos, L. R., and Polonelli, L. (2009) Antibodies as crypts of antiinfective and antitumor peptides. *Curr. Med. Chem.* **16,** 2305–2323
13. Xu, J. L., and Davis, M. M. (2000) Diversity in the CDR3 region of V_H is sufficient for most antibody specificities. *Immunity* **13,** 37–45
14. Levi, M., Sällberg, M., Rudén, U., Herlyn, D., Maruyama, H., Wigzell, H., Marks, J., and Wahren, B. (1993) A complementarity-determining region synthetic peptide acts as a miniantibody and neutralizes human immunodeficient virus type 1 *in vitro*. *Proc. Natl. Acad. Sci. U.S.A.* **90,** 4374–4378
15. Heap, C. J., Wang, Y., Pinheiro, T. J., Reading, S. A., Jennings, K. R., and Dimmock, N. J. (2005) Analysis of a 17-amino acid residue, virus-neutralizing microantibody. *J. Gen. Virol.* **86,** 1791–1800
16. Dobroff, A. S., Rodrigues, E. G., Juliano, M. A., Friaça, D. M., Nakayasu, E. S., Almeida, I. C., Mortara, R. A., Jacysyn, J. F., Amarante-Mendes, G. P., Magliani, W., Conti, S., Polonelli, L., and Travassos, L. R. (2010) Differential antitumor effects of IgG and IgM monoclonal antibodies and their synthetic complementarity-determining regions directed to new targets of B16F10-Nex2 melanoma cells. *Transl. Oncol.* **3,** 204–217
17. Dobroff, A. S., Rodrigues, E. G., Moraes, J. Z., and Travassos, L. R. (2002) Protective, anti-tumor monoclonal antibody recognizes a conformational epitope similar to melibiose at the surface of invasive murine melanoma cells. *Hybrid. Hybridomics* **21,** 321–331
18. Murray, D., Mirzayans, R., Scott, A. L., and Allalunis-Turner, M. J. (2003) Influence of oxygen on the radiosensitivity of human glioma cell lines. *Am. J. Clin. Oncol.* **26,** e169–177
19. Buonassisi, V., and Venter, J. C. (1976) Hormone and neurotransmitter receptors in an established vascular endothelial cell line. *Proc. Natl. Acad. Sci. U.S.A.* **73,** 1612–1616
20. Shevchenko, A., Wilm, M., Vorm, O., and Mann, M. (1996) Mass spectrometric sequencing of proteins silver-stained polyacrylamide gels. *Anal. Chem.* **68,** 850–858
21. Moragues, M. D., Omaetxebarria, M. J., Elguezabal, N., Sevilla, M. J., Conti, S., Polonelli, L., and Pontón, J. (2003) A monoclonal antibody directed against a *Candida albicans* cell wall mannoprotein exerts three anti-*C. albicans* activities. *Infect. Immun.* **71,** 5273–5279
22. Gourlay, C. W., and Ayscough, K. R. (2005) The actin cytoskeleton: a key regulator of apoptosis and ageing? *Nat. Rev. Mol. Cell. Biol.* **6,** 583–589
23. Gruenbaum, Y., Goldman, R. D., Meyuhas, R., Mills, E., Margalit, A., Fridkin, A., Dayani, Y., Prokocimer, M., and Enosh, A. (2003) The nuclear lamina and its functions in the nucleus. *Int. Rev. Cytol.* **226,** 1–62
24. Kim, B. M., Choi, Y. J., Han, Y., Yun, Y. S., and Hong, S. H. (2009) *N,N*-Dimethyl phytosphingosine induces caspase-8-dependent cytochrome *c* release and apoptosis through ROS generation in human leukemia cells. *Toxicol. Appl. Pharmacol.* **239,** 87–97
25. Gomes, A., Bhattacharjee, P., Mishra, R., Biswas, A. K., Dasgupta, S. C., and Giri, B. (2010) Anticancer potential of animal venoms and toxins. *Indian J. Exp. Biol.* **48,** 93–103
26. Chernysh, S., Kim, S. I., Bekker, G., Pleskach, V. A., Filatova, N. A., Anikin, V. B., Platonov, V. G., and Bulet, P. (2002) Antiviral and antitumor peptides from insects. *Proc. Natl. Acad. Sci. U.S.A.* **99,** 12628–12632
27. Cozzolino, R., Palladino, P., Rossi, F., Calì, G., Benedetti, E., and Laccetti, P. (2005) Antineoplastic cyclic astin analogues kill tumour cells via caspase-mediated induction of apoptosis. *Carcinogenesis* **26,** 733–739
28. Chen, J. Y., Lin, W. J., Wu, J. L., Her, G. M., and Hui, C. F. (2009) Epinecidin-1 peptide induces apoptosis which enhances antitumor effects in human leukemia U937 cells. *Peptides* **30,** 2365–2373
29. Sato, M., Sagawa, M., Nakazato, T., Ikeda, Y., and Kizaki, M. (2007) A natural peptide, dolastatin 15, induces G_2/M cell cycle arrest and apoptosis of human multiple myeloma cells. *Int. J. Oncol.* **30,** 1453–1459
30. Barras, D., and Widmann, C. (2011) Promises of apoptosis-inducing peptides in cancer therapeutics. *Curr. Pharm. Biotechnol.* **12,** 1153–1165
31. Levee, M. G., Dabrowska, M. I., Lelli, J. L., Jr., and Hinshaw, D. B. (1996) Actin polymerization and depolymerization during apoptosis in HL-60 cells. *Am. J. Physiol. Cell Physiol.* **271,** C1981–1992
32. Posey, S. C., and Bierer, B. E. (1999) Actin stabilization by jasplakinolide enhances apoptosis induced by cytokine deprivation. *J. Biol. Chem.* **274,** 4259–4265
33. Odaka, C., Sanders, M. L., and Crews, P. (2000) Jasplakinolide induces apoptosis in various transformed cell lines by a caspase-3-like protease-dependent pathway. *Clin. Diagn. Lab. Immunol.* **7,** 947–952
34. Rao, J. Y., Jin, Y. S., Zheng, Q., Cheng, J., Tai, J., and Hemstreet, G. P., 3rd (1999) Alterations of the actin polymerization status as an apoptotic morphological effector in HL-60 cells. *J. Cell. Biochem.* **75,** 686–697
35. Franklin-Tong, V. E., and Gourlay, C. W. (2008) A role for actin in regulating apoptosis/programmed cell death: evidence spanning yeast, plants and animals. *Biochem. J.* **413,** 389–404
36. Wang, H., Schultz, R., Hong, J., Cundiff, D. L., Jiang, K., and Soff, G. A. (2004) Cell surface-dependent generation of angiostatin4.5. *Cancer Res.* **64,** 162–168
37. Miles, L. A., Andronicos, N. M., Baik, N., and Parmer, R. J. (2006) Cell-surface actin binds plasminogen and modulates neurotransmitter release from catecholaminergic cells. *J. Neurosci.* **26,** 13017–13024
38. Moroianu, J., Fett, J. W., Riordan, J. F., and Vallee, B. L. (1993) Actin is a surface component of calf pulmonary artery endothelial cells in culture. *Proc. Natl. Acad. Sci. U.S.A.* **90,** 3815–3819
39. Owen, M. J., Auger, J., Barber, B. H., Edwards, A. J., Walsh, F. S., and Crumpton, M. J. (1978) Actin may be present on the lymphocyte surface. *Proc. Natl. Acad. Sci. U.S.A.* **75,** 4484–4488
40. Sanders, S. K., and Craig, S. W. (1983) A lymphocyte cell surface molecule that is antigenically related to actin. *J. Immunol.* **131,** 370–377
41. Tang, H. L., Le, A. H., and Lung, H. L. (2006) The increase in mitochondrial association with actin precedes Bax translocation in apoptosis. *Biochem. J.* **396,** 1–5
42. DesMarais, V., Ghosh, M., Eddy, R., and Condeelis, J. (2005) Cofilin takes the lead. *J. Cell Sci.* **118,** 19–26
43. Chua, B. T., Volbracht, C., Tan, K. O., Li, R., Yu, V. C., and Li, P. (2003) Mitochondrial translocation of cofilin is an early step in apoptosis induction. *Nat. Cell Biol.* **5,** 1083–1089
44. Leadsham, J. E., Kotiadis, V. N., Tarrant, D. J., and Gourlay, C. W. (2010) Apoptosis and the yeast actin cytoskeleton. *Cell Death Differ.* **17,** 754–762
45. Giammarioli, A. M., Maselli, A., Casagrande, A., Gambardella, L., Gallina, A., Spada, M., Giovannetti, A., Proietti, E., Malorni, W., and Pierdominici, M. (2008) Pyrimethamine induces apoptosis of melanoma cells via a caspase and cathepsin double-edged mechanism. *Cancer Res.* **68,** 5291–5300

β-Actin-binding Complementarity-determining Region 2 of Variable Heavy Chain from Monoclonal Antibody C7 Induces Apoptosis in Several Human Tumor Cells and Is Protective against Metastatic Melanoma

Denise C. Arruda, Luana C. P. Santos, Filipe M. Melo, Felipe V. Pereira, Carlos R. Figueiredo, Alisson L. Matsuo, Renato A. Mortara, Maria A. Juliano, Elaine G. Rodrigues, Andrey S. Dobroff, Luciano Polonelli and Luiz R. Travassos

J. Biol. Chem. 2012, 287:14912-14922.
doi: 10.1074/jbc.M111.322362 originally published online February 13, 2012
